NUREG/CR-0800
PNL-2977
R5

Estimate of Feasibility to Develop Acoustic Emission—Flaw Relationships for Inservice Monitoring of Nuclear Pressure Vessels

P. H. Hutton
E. B. Schwenk
R. J. Kurtz

April 1979

Prepared for
the U.S. Nuclear Regulatory Commission

Pacific Northwest Laboratory
Operated for the U.S. Department of Energy
by Battelle Memorial Institute

Battelle

PNL-2977

NOTICE

PACIFIC NORTHWEST LABORATORY
operated by
BATTELLE
for the
UNITED STATES DEPARTMENT OF ENERGY
Under Contract EY-76-C-06-1830

Printed in the United States of America
Available from
National Technical Information Service
United States Department of Commerce
5285 Port Royal Road
Springfield, Virginia 22151

Price: Printed Copy $____*; Microfiche $3.00

*Pages	NTIS Selling Price
001-025	$4.00
026-050	$4.50
051-075	$5.25
076-100	$6.00
101-125	$6.50
126-150	$7.25
151-175	$8.00
176-200	$9.00
201-225	$9.25
226-250	$9.50
251-275	$10.75
276-300	$11.00

NUREG/CR - 0800
PNL - 2977
R5

ESTIMATE OF FEASIBILITY TO DEVELOP ACOUSTIC EMISSION--FLAW RELATIONSHIPS FOR INSERVICE MONITORING OF NUCLEAR PRESSURE VESSELS

P. H. Hutton
E. B. Schwenk
R. J. Kurtz

April 1979

Prepared for
the U.S. Nuclear Regulatory Commission
under a Related Services Agreement
with the U.S. Department of Energy
Contract EY-76-C-06-1830
FIN NO. B2088

Pacific Northwest Laboratory
Richland, Washington 99352

ESTIMATE OF FEASIBILITY TO DEVELOP ACOUSTIC EMISSION--FLAW RELATIONSHIPS FOR INSERVICE MONITORING OF NUCLEAR PRESSURE VESSELS

EXECUTIVE SUMMARY

The work presented in this report is part of an ongoing program at Pacific Northwest Laboratory to determine the feasibility of continuous inservice monitoring of nuclear pressure vessels, using acoustic emission (AE) to detect and evaluate growing flaws. The work is sponsored by the Reactor Safety Research Division of the United States Nuclear Regulatory Commission. The major program objectives are to:

- develop criteria to distinguish flaw growth AE from nonsignificant acoustic signals
- develop an AE/flaw growth model as a basis for relating inservice AE to flaw significance
- demonstrate application of program results through both off-reactor and on-reactor testing.

This work was initiated in July 1976, with most of the preliminary activity aimed at developing appropriate AE measurement methods. Subsequent emphasis was placed on developing AE/flaw relationships, which is one of the major program objectives.

To fulfill the program objectives, laboratory fracture mechanics tests have been performed. These tests were designed to determine the effect of variables such as microstructure, flaw geometry, temperature and mechanical loading upon the AE response during increasing flaw severity. Future tests will more fully simulate reactor pressure vessel behavior.

From these tests, two empirical models have been developed to relate AE to fatigue crack growth. One model relates rate of change of AE to stress intensity factor range or the crack growth rate. The other model relates

total accumulated AE to stress intensity factor. Both of these are still preliminary models that need refinement. They do, however, demonstrate for 14 variations in material, geometry and temperature (collectively) a consistent increase in AE associated with increasing flaw severity. The results thus far are encouraging and we conclude that there is a high potential for achieving the goal of detecting and evaluating flaw growth in a reactor pressure vessel by continuous AE monitoring.

Further assessment of feasibility hinges upon the results of tests designed to more fully simulate the reactor pressure vessel. These tests (to be performed during the latter half of FY-79 and FY-80) will consist of experiments incorporating heavy section material and include environmental factors such as high-temperature and high-pressure water in contact with a growing crack.

CONTENTS

FIGURES

FIGURES (cont'd)

TABLES

ESTIMATE OF FEASIBILITY TO DEVELOP ACOUSTIC EMISSION--FLAW RELATIONSHIPS FOR INSERVICE MONITORING OF NUCLEAR PRESSURE VESSELS

INTRODUCTION

The purpose of this program is to evaluate the feasibility of detecting and analyzing flaw growth in reactor pressure boundaries by continuously monitoring for acoustic emission (AE). Major program objectives are:

- develop criteria to distinguish flaw growth AE from nonsignificant acoustic signals
- develop an AE/flaw growth model as a basis for relating inservice AE to flaw significance
- demonstrate application of program results through both off-reactor and on-reactor testing.

The program was initiated in July 1976. One of the identified requirements is an evaluation of feasibility of achieving the program objectives based on results through FY-78. This report presents that evaluation and recommends additional investigation required. The time period covered has been extended into FY-79 to permit including important test results.

SUMMARY

To fulfill the program objectives, laboratory fracture mechanics tests have been performed. These tests were designed to determine the effect of variables such as microstructure, flaw geometry, temperature and mechanical loading upon the AE response during increasing flaw severity. The results of these tests consistently show that an increased AE response is associated with increasing flaw severity. Thus, we conclude that there is a high potential for achieving the goal of detecting and evaluating flaw growth in a reactor pressure vessel by continuous AE monitoring.

Achieving the potential of detecting and evaluating flaw growth in a reactor pressure vessel depends upon two major factors: first, consistent relationships between flaw severity and measurable AE parameters and, second, a data acquisition system suitable for long term exposure to a reactor environment.

The first factor includes characterization of significant AE and development of an AE/flaw growth model (the first two program objectives). Primary emphasis has been on developing an AE/flaw growth model using laboratory fracture mechanics scoping tests.

Two major mechanical loading conditions were considered for the preliminary scoping tests on A533B material. The first was associated with the assumption that fatigue crack growth (FCG) is the primary mechanism whereby flaws grow in a pressure vessel during service. Secondly, it was decided that transient loading conditions should be considered if the approach was to have application to, for example, off-normal reactor operation. Hence, laboratory FCG and fracture (rising load) testing were incorporated into the program. The parameters for FCG and fracture tests on A533B material have been monitored for AE at room temperature and 550^{o}F in air. Three laboratory specimen configurations were used to gather the appropriate information: 1) single edge notch (SEN)-through wall, 2) part-through wall surface notch (SN), and 3) compact tension (CT)-through wall.

The AE results from these tests and the results from two heavy section steel technology (HSST) pressure vessel tes s (6 in. wall thickness) were compared to assess the potential feasibility of using AE to monitor flaw growth in nuclear pressure vessels. In general, AE increased with flaw severity for al: tests. Most of the AE response from SEN defect fracture tests occurred after maximum load was reached; hence, the majority of the AE probably occurred from ductile crack extension during mechanical instability. The data from the SN defect fracture tests at room temperature and 550°F correlated well in form with the HSST pressure vessel tests at -5° and 200°F, and the AE response appeared to be independent of temperature over the temperature ranges tested. The SN defect laboratory fracture tests and the HSST tests were philosophically similar in that both employed part-through wall defects and they were mechanically loaded in a similar manner.

The laboratory FCG tests with both SEN and SN defects showed a temperature effect. Crack growth rates at 550°F for the SEN defects were between 55% and 75% higher than at room temperature for the same stress intensity factor range (ΔK); but the AE produced per cycle for the same crack growth rate appears to be less for the higher temperature. The limited SN data were similar to the SEN results.

A limited number of results were obtained from CT specimens fabricated out of base and weld metal. The microstructural difference between the two specimens did not yield a significant difference in the AE behavior at room temperature.

One slag inclusion test was performed giving an AE response 4-1 ? times larger than that of a control sample. However, the results were inc clusive to distinguish slag cracking from metal cracking AE within the scope of the parameters measured. This may be due to the relative smallness of the slag inclusion and incomplete fusion associat d with the specimen weld.

Four available high-temperature AE sensors have been tested for 2830 hr exposure at 500° to 550°F in air with weekly cycling to room temperature. Results show that two sensors (a metal waveguide and a direct surface contact sensor) can withstand high-temperature environment for an extended period.

567 023

One AE characterization test was completed which showed a decrease in AE (particularly high-amplitude signals) upon immersion of the specimen in water. The reason for this effect is being investigated. This same specimen was used to investigate the effects of an oxide on the crack surface. When compared to AE from FCG in the same specimen prior to oxidation, the "oxide data" showed a higher AE rate than data obtained from unoxidized specimens until the fatigue crack front moved away from the oxidized fracture surface. At this point, the AE rate returned to levels similar to that obtained prior to oxidation.

The successful application of AE to pressure vessel monitoring depends upon consistent relationships between flaw severity and measurable AE parameters. Two empirical models have been developed to relate AE to FCG. One model relates rate of change of AE to ΔK or the crack growth rate (da/dn). The other model relates total accumulated AE to K. Both of these are still preliminary models that need refinement. They do, however, demonstrate for 14 variations in material, geometry and temperature (collectively) a consistent increase in AE associated with an increasing flaw severity. In addition, three theoretical models based upon linear elastic fracture mechanics were compared against the FCG results obtained from several different specimens. Only limited promise with such models was found. Room temperature SEN-FCG data correlated with plastic zone area and crack area models, while CT data correlated with the plastic zone volume model. The 550^{o}F data could not be correlated with any of the three theoretical models.

Analysis of measured AE signal parameters--energy, peak-time, amplitude, and first half-cycle polarity--has not shown clear AE signal characterization. Very preliminary results using pattern recognition techniques are encouraging.

The overall results thus far are favorable and the program objectives appear feasible and practical. We believe that continuing research is necessary in the following areas to achieve program objectives:

1. Continued development and verification of the AE/flaw model through further investigation of the influence of load cycle rate, R-ratio, simulated service loading, material volume, flaw geometry, temperature, and water on AE in flawed heavy section material.

2. Development of AE signal characterization through more rigorous analysis of the AE signal waveform including such parameters as energy, a modified measure of peak-time and amplitude during FCG, and time location of the AE signal with respect to the load waveform (a new parameter). Pattern recognition techniques need to be further investigated as a potential method of AE signal identification.

3. Continued development of data acquisition methodology through AE sensor testing in a true reactor environment.

4. Design of an optimized on-reactor AE data acquisition system.

5. Design of a methodology for application of an interpretive model in the field.

TEST RESULTS AND ANALYSIS

FATIGUE CRACK GROWTH

A number of FCG tests of A533B base and weld metal have been performed at room temperature and 550°F and monitored for AE. Several specimen geometry and material property variations have been investigated. A summary of the FCG conditions employed is given in Table 1. The fatigue crack growth rate (da/dn) versus stress intensity factor range (ΔK) data for three room temperature tests are plotted in Figure 1. Within the range of normal experimental scatter, all of the room temperature da/dn versus ΔK data fell on the same curve. The 550°F crack growth rate was between 55% and 75% higher than the room temperature crack growth rate for the same ΔK level (dashed line in Figure 1, no data points included).

In general, AE-FCG data from all specimens behaved consistently. The rate of change of AE increased with increases in either da/dn or ΔK. Plots of the AE event count rate (counts/cycle, dN/dn) versus da/dn are given in Figures 2 to 5.

The SEN results plotted in Figure 2 show the effects of temperature and prior plastic strain upon the AE data rate. While the 550°F data represent only one specimen, increasing temperature appears to decrease the amount of AE produced per cycle for the same da/dn.

Limited experimental work on the effect of R ratio ($R = P_{min}/P_{max}$) was obtained during the 550°F FCG test. The results (Figure 2) are inconclusive as to the effect of R ratio at 550°F, since they fall within the SEN-FCG data scatter band. SEN specimen 1-1A-2A was longitudinally prestrained. Again, the results do not illustrate a distinctive effect since they fall within the general data scatter band.

Results obtained from compact tension (2T-CT) specimens fabricated from base and weld metal are plotted in Figure 3. The microstructural difference between the two specimens did not produce a significant difference in the AE rate behavior.

TABLE 1. Summary of Fatigue Crack Growth Test Conditions for A533B Cl 1 Steel

Specimen No.	Specimen Type	Thickness, in.	Test Temp, °F	Material Condition	R Ratio	Rate, Hz	AE System Sensitivity, μbar	Comments
B2-1B	2T-CT	1.75	RT	BM[a]	0.1	3	0.11	
B2-1A	2T-CT	1.75	RT	WM[b]	0.1	3	0.09	
1-1A-2A	SEN	0.5	RT	BM		1-4	0.08	3% Prestrain
1-2A-1B	SEN	1.0	RT	BM	0.1	2-3	0.11	3 Pt. Bend
1-2A-2B	SEN	1.0	RT	BM	0.1	3-10	0.11	Straightened
1-2A-6B	SEN	1.0	550	BM	0.1, 0.5	2-3	0.9	
2-1A-2B	SN	1.0	RT	BM	0.1	1-2	0.11	3 Pt. Bend
1-2A-6A	SN	1.0	RT, 550	BM	0.1	1	0.12	Straightened

(a) BM = Base Metal
(b) WM = Weld Metal

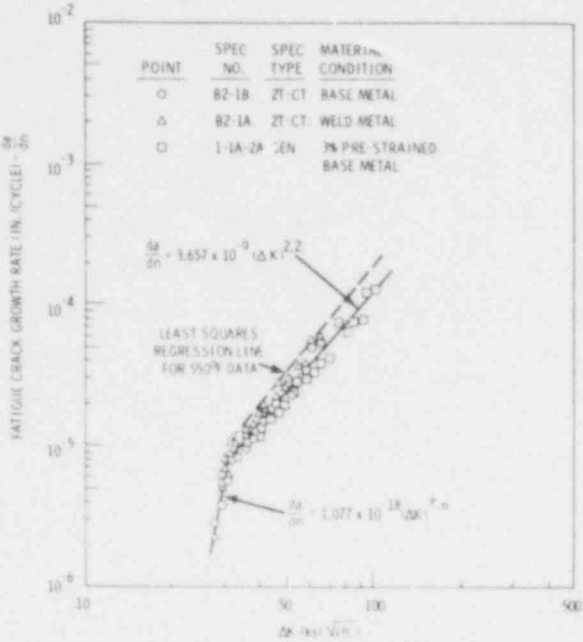

FIGURE 1. Fatigue Crack Growth Rate (da/dn) Versus Stress Intensity Factor Range (ΔK) for Three Fatigue Specimens (R=0.1, 3Hz)

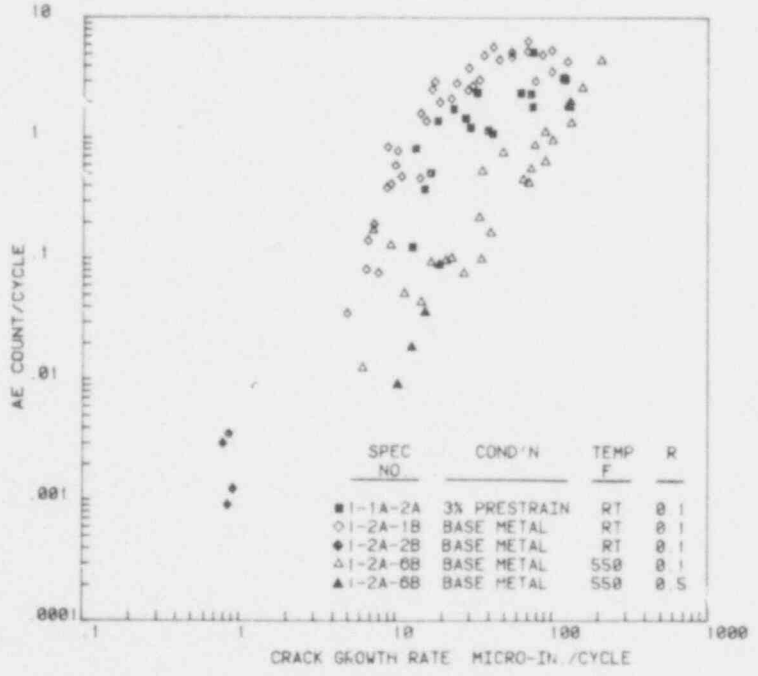

FIGURE 2. AE Rate Versus Fatigue Crack Growth Rate for SEN Type Specimens

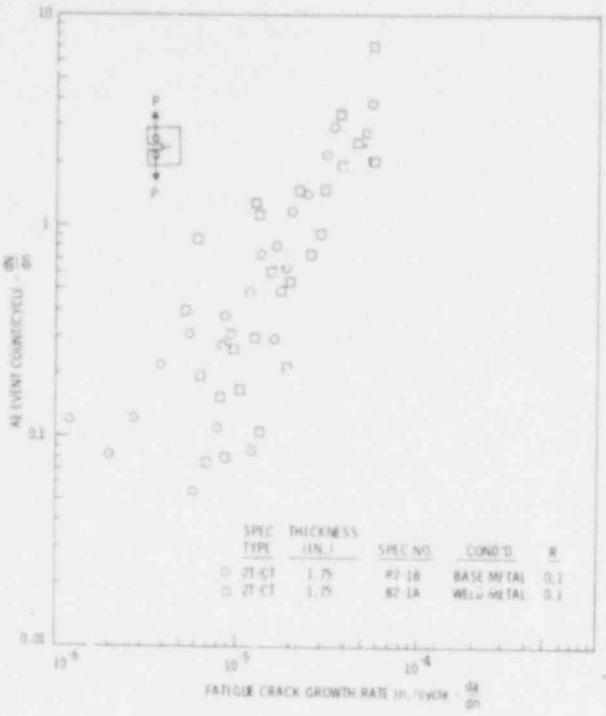

FIGURE 3. AE Rate Versus Fatigue Crack Growth Rate for 2T-CT Type Specimens

Experimental data obtained during room temperature and 550°F FCG of two SN specimens are plotted in Figure 4. The effect of temperature on the AE rate was not as definite as for the SFN defect specimens, but the same general trend appears. Note that the AE rate drops off markedly as the net section stress approaches the 550°F yield strength. This effect has also been observed on the room temperature SEN-FCG tests.(1)

Another interesting effect observed during room temperature FCG testing of SN specimen 1-2A-6A was the apparent initially decreasing AE rate with increasing da/dn. This may have been due to buildup of oxide on the fatigue crack fracture surfaces resulting from the abnormal test sequence applied to this specimen. The specimen was notched and fatigue cycled just long enough to initiate a fatigue crack. Then, because of other program demands upon the AE monitoring equipment, the specimen was set aside for several months. During that time, the notch was covered, but not sealed from the laboratory atmosphere. Thus, oxidation of the fatigue crack fracture surfaces was probably occurring during the extended storage in the lab. Assuming that much of the initial AE was caused by oxidation effects, then the decreasing AE rate

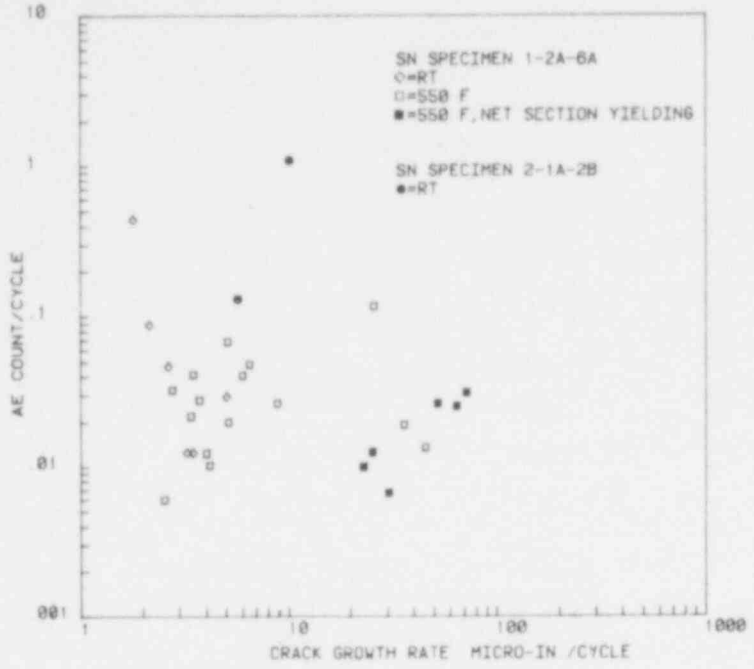

FIGURE 4. AE Rate Versus Fatigue Crack Growth Rate for SN Type Specimens (R= 0.1)

with increasing crack growth is attributed to movement of the crack front away from the oxidized fracture surfaces. For more evidence of this effect, see the Characterizations Section.

To compare the effect of defect geometry upon the AE rate, a composite plot of all FCG data is shown in Figure 5. The composite plot was constructed from the data in Figures 2 to 4. Each defect type is distinguished by a seperate color as noted in Figure 5. The results indicate no significant differences between the various defect geometries. This contrasts with the fracture test results which do tend to depend upon the defect geometry.

FRACTURE

Fracture tests on laboratory specimens and 6-in-thick, intermediate-scale, HSST pressure vessels,[2,3] have also been monitored using AE. The fracture test conditions are summarized in Table 2. The laboratory test results are plotted in Figures 6 to 13 and the vessel test data are shown in Figures 14 and 15. The AE-fracture test results for all test conditions show that AE response increases with flaw severity.

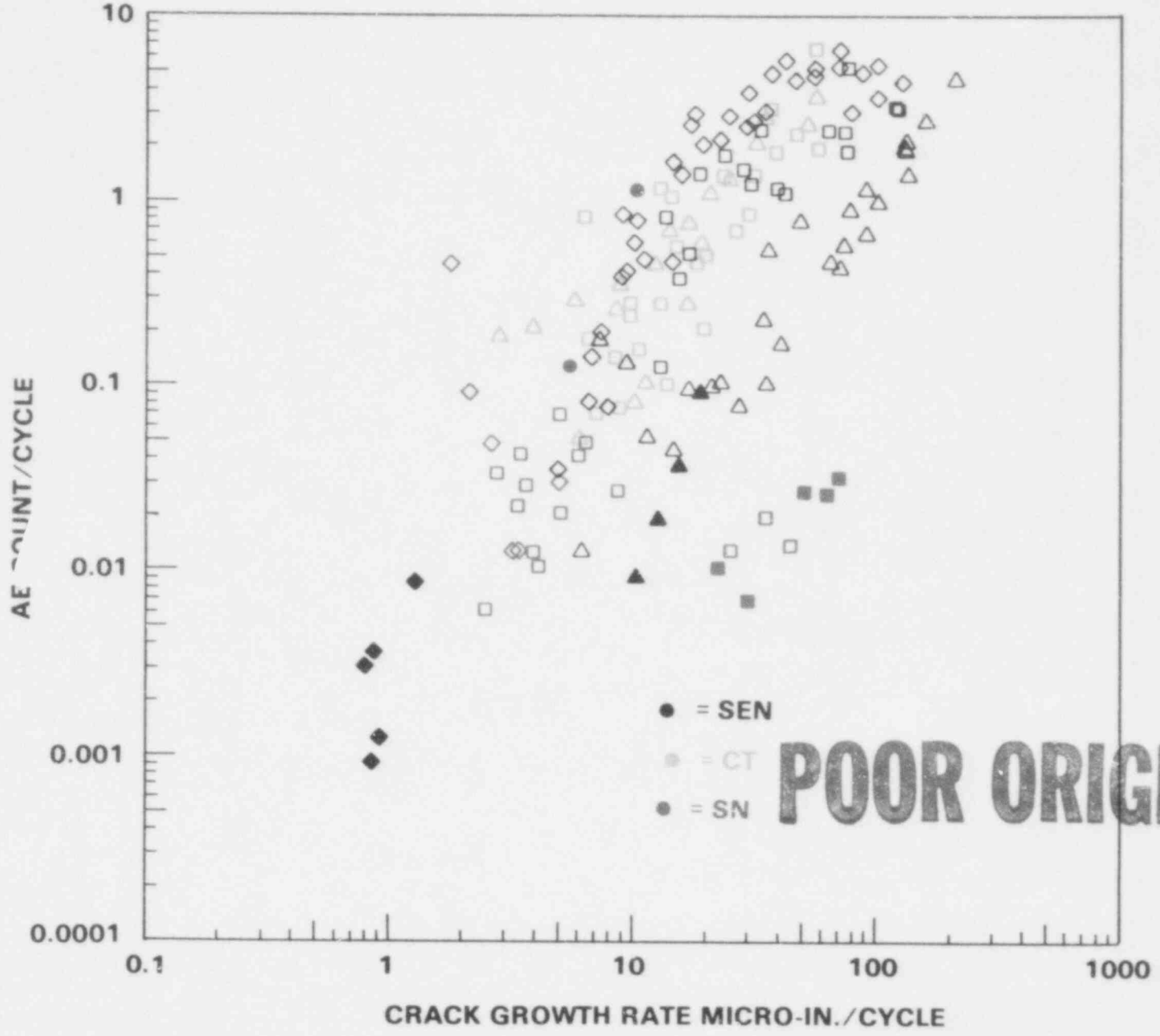

FIGURE 5. AE Rate Versus Fatigue Crack Growth Rate for SEN, 2T-CT, and SN Type Specimens

TABLE 2. Summary of Fracture Test Conditions for A533B Cl 1 Steel

Specimen No.	Specimen Type	Thickness, in.	Test Temp, ^{o}F	Material Condition	AE System Sensitivity, μbar	Comments
B2-1B	2T-CT	1.75	RT	BM[a]	0.11	Prior RT FCG
B2-3A	2T-CT	1.75	RT	WM[b]	0.16	RT Fatigue Precracked
B2-3B	2T-CT	1.75	RT	BM	0.19	RT Fatigue Precracked
1-2A-2B	SEN	1.0	RT	BM	0.11	Prior RT FCG
2-1A-2B	SN	1.0	RT	BM	0.11	3 Pt. Bend Straightened Prior RT FCG
1-2A-6B	SEN	1.0	550	BM	0.09	Prior 550^{o}F FCG
V7-B	VESSEL	6.0	200	WM	0.14	HSST Test EB[c] Weld Precracked
ITV-8	VESSEL	6.0	-5	WM	0.20	HSST Test RT Fatigue Precracked

(a) BM = Base Metal
(b) WM = Weld Metal
(c) EB = Electron Beam

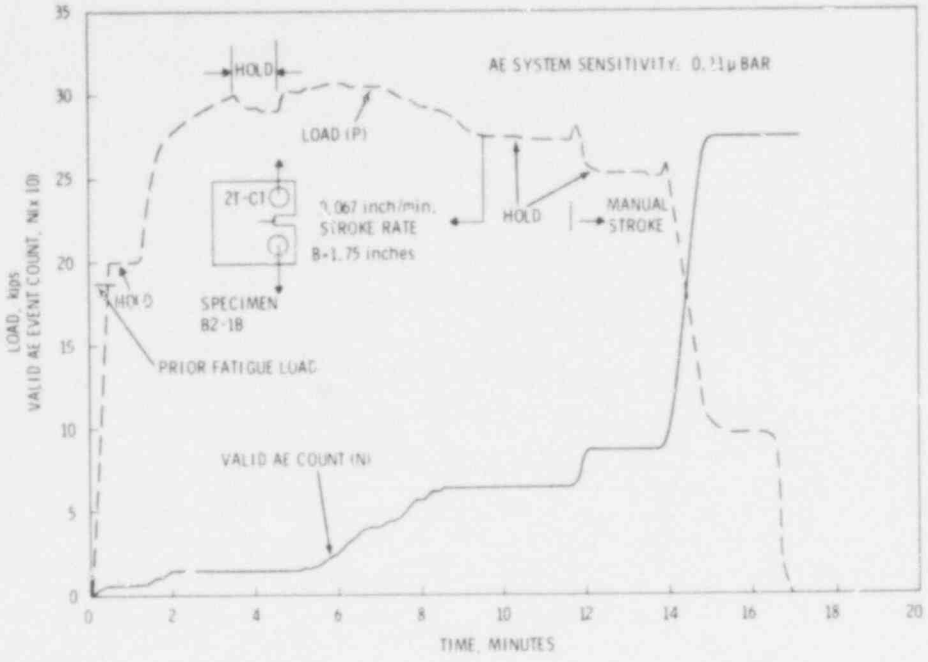

FIGURE 6. Fracture Test B2-1B Data--Base Metal

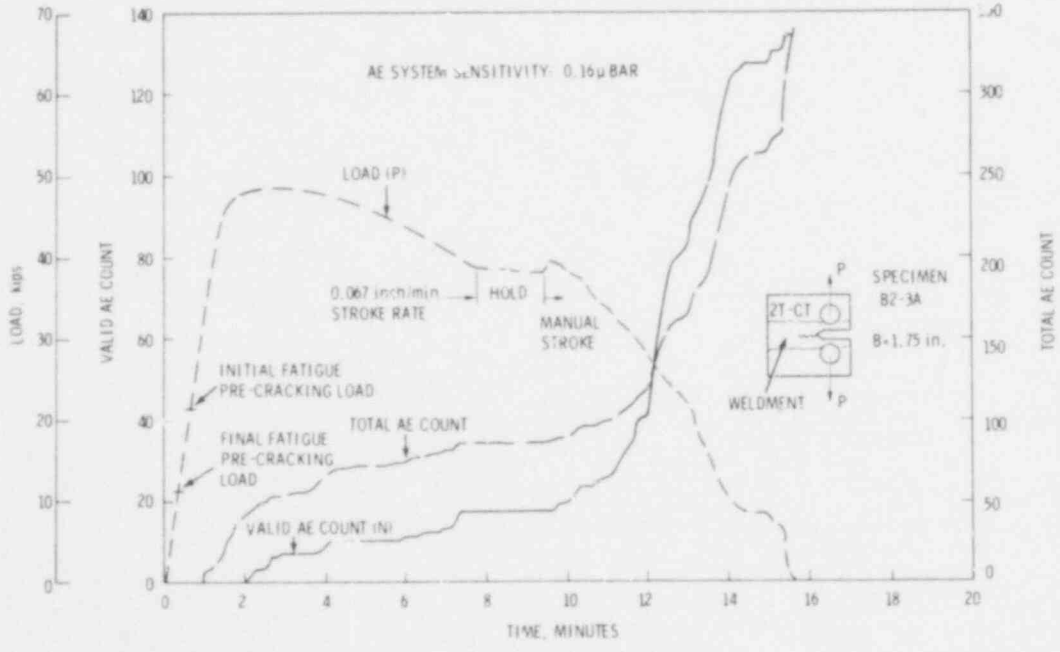

FIGURE 7. Fracture Test B2-3A Data--Weld Metal

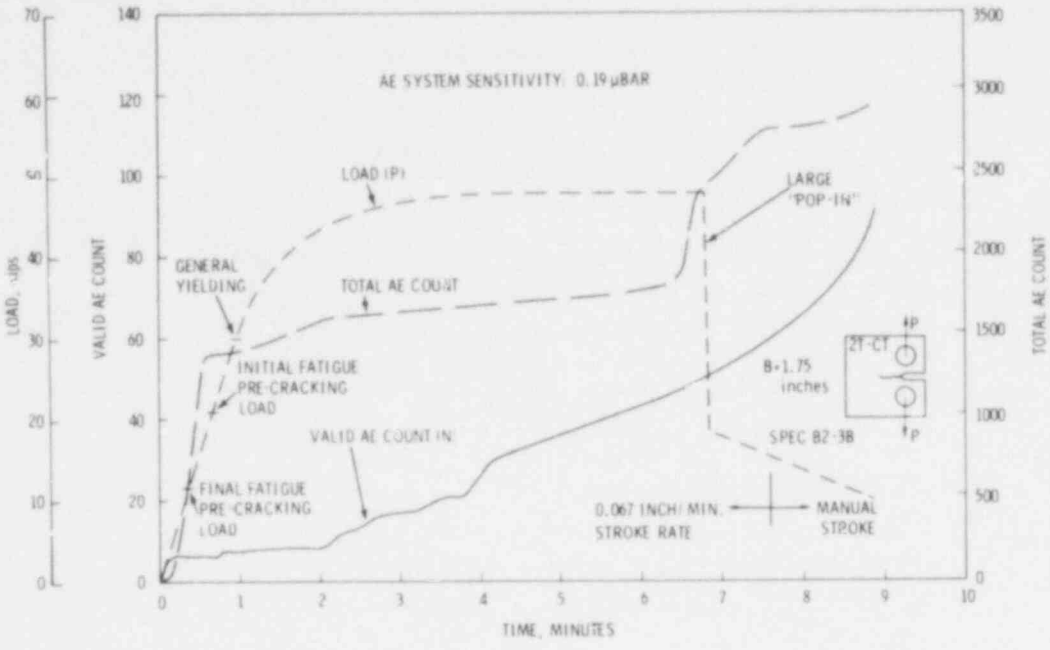

FIGURE 8. Fracture Test B2-3B Data--Base Metal

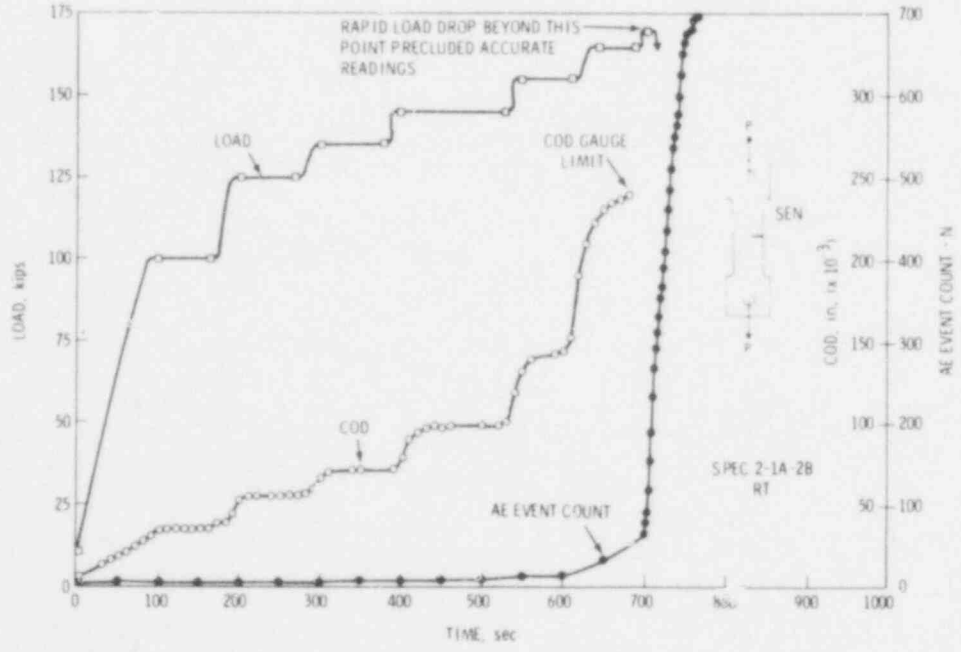

FIGURE 9. Load, COD and AE Event Count Versus Time, Specimen 1-2A-2B, Room Temperature. (Maximum final fatigue pre-crack load was 15 kip)

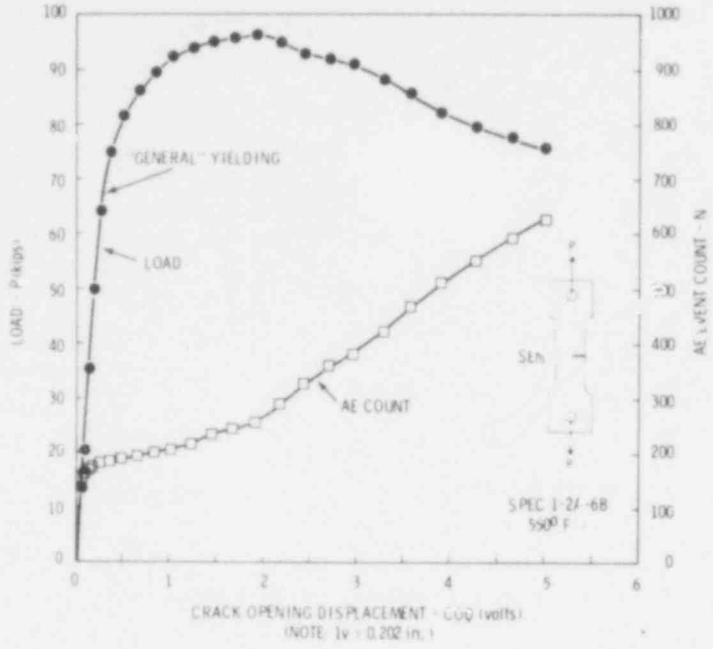

FIGURE 10. Load and AE Event Count Versus COD, SEN Specimen 1-2A-6B, 550°F

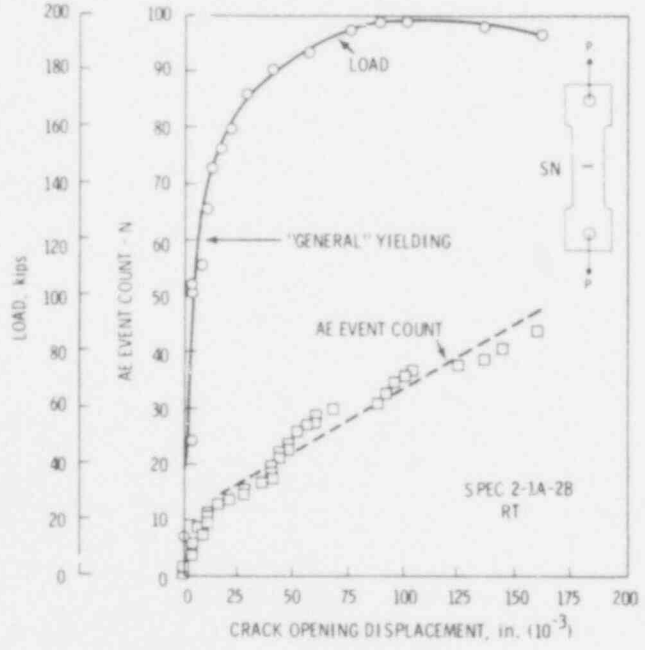

FIGURE 11. Load and AE Event Count Versus COD, SN Specimen 2-1A-2B, Room Temperature

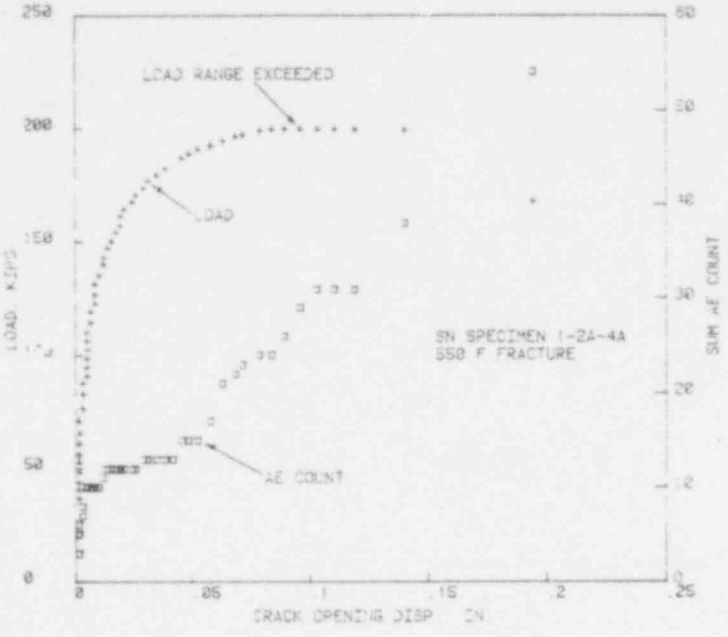

FIGURE 12. Load and AE Event Count Versus COD, SN Specimen 1-2A-4A, 550°F

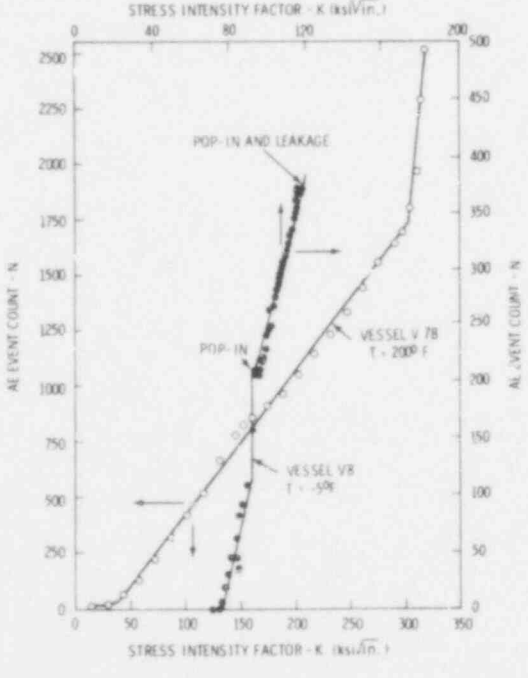

FIGURE 13. Summation AE Versus K for Vessel V7-B (200°F) and V8 (-5°F)

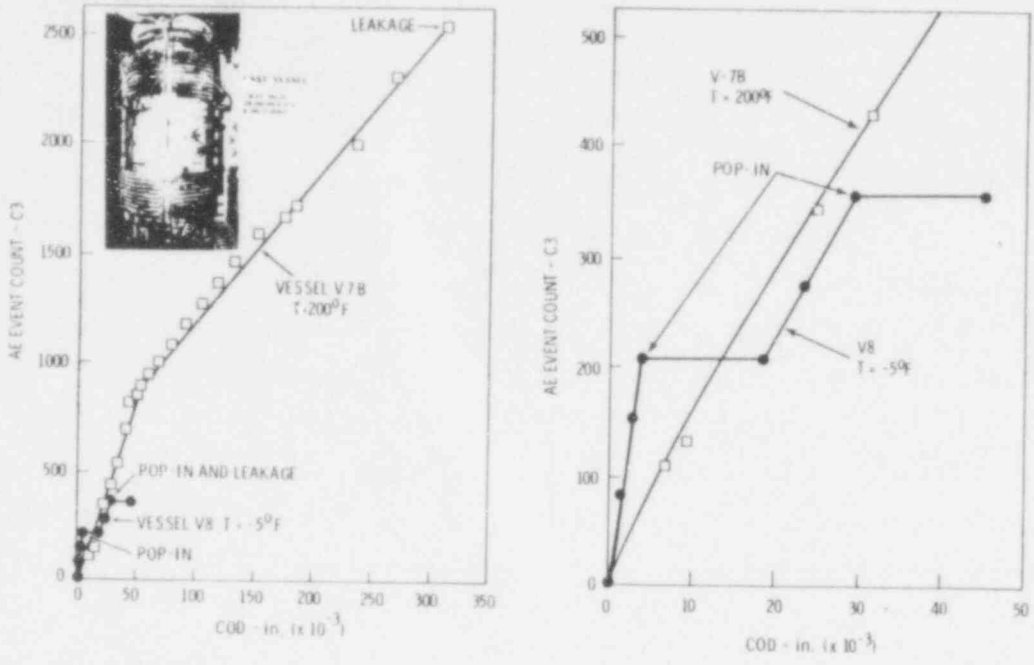

FIGURE 14. Summation AE Versus COD for Vessel V7-B (200°F) and V8 (-5°F)

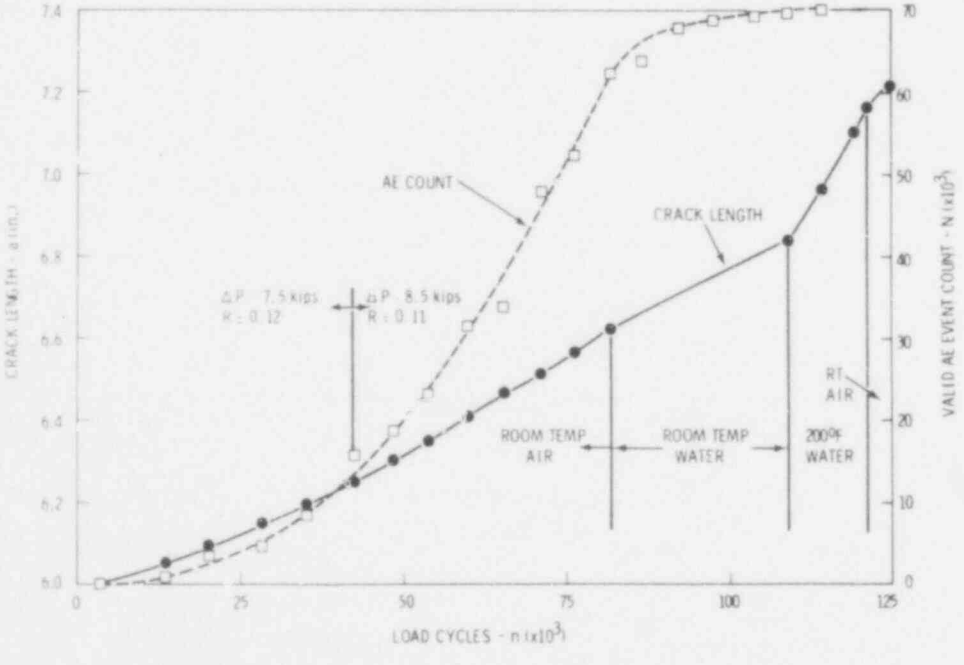

FIGURE 15. Crack Growth and AE Versus Load Cycles for Fatigue Crack Growth in Air and Water

The fracture specimens tested at room temperature and 550°F with through-wall crack geometries (2T-CT and SEN), shown in Figures 6 to 10, generally produced very little AE during the elastic and early plastic portions of the loading. Most of the AE from these specimens was detected after the maximum load was exceeded and therefore, occurred from ductile crack extension during mechanical instability. The 550°F fracture test (Figure 10) showed a greater amount of AE than room temperature tests but still displayed the same pattern as the room temperature-SEN results. This result shows a temperature effect upon the AE obtained during fracture opposite to the one observed during FCG. No explanation for this test has been established; however, from post-test inspection, it appears to be possible that a heat shield touched the specimen near the flaw, causing noise signals to be recorded as valid AE.

Two fracture tests (one at room temperature and one at 550°F) were conducted on specimens with part-through wall SN configurations, which yielded results different from the through-wall data (see Figures 11 and 12). In these instances, AE was detected both before and after general yielding, with linear AE versus crack opening displacement (COD) relationships up to general yielding and between yielding and failure. These results are analogous to the HSST vessel tests (see Figures 13 and 14) in the following ways: (1) the general shapes of the AE-COD plots are similar; (2) both the lab and vessel data show negligible effect of temperature on detected AE; and (3) the crack and loading geometry are similar.

During both of the vessel tests, the AE accumulated in a manner that indicated the feasibility of monitoring large structures. First, the AE accumulation consistently increased with increasing flaw severity, as measured by K and COD. Moreover, pop-in precursor activity was also detected, indicating a sensitivity to relatively small amounts of plasticity and/or crack extensions that occur prior to the relatively large pop-in crack extensions. It should be noted that K in Figure 13 was calculated based on original flaw dimensions. Information on the shift in K associated with the pop-in in vessel V8 is not yet available. During the most dynamic part of the pop-ins (including leakage) where the signal density was very high (as observed

on an oscilloscope), the AE system locked out. This was due to a design feature to avoid multiple counts from one signal. A different design commonly used in field monitoring systems would have shown a very sharp increase in response to the high-density data, thus providing a bench mark to signify occurrence of a pop-in.

The AE-COD curves for both vessel tests (Figure 14) remained linear to failure (leakage) even though, in the case of the 200°F test, significant crack extension was occurring near the end of the test, as suggested by the AE-K curve (Figure 13). The fact that the COD seems to correlate more effectively than K with AE during fracture indicates that flaw damage models based strictly on linear elastic fracture mechanics may not adequately model the data. However, the laboratory SN and HSST results indicate AE response to be a feasible method for monitoring the flaw severity of part-through cracks in large structures.

CHARACTERIZATIONS

The analysis of measured AE signal parameters from various sources--energy, peak time, amplitude, first half-cycle polarity--has not shown any consistent characterization. New approaches to AE characterization are planned as discussed under recommendations for future work.

A double cantilever beam (DCB) specimen was used to investigate the effects of water on AE from FCG. The results (Figure 15) showed a decrease in AE (particularly high-amplitude signals) upon immersion of the specimen in water. The decrease in detected AE could be due to surface wave damping by water, dissipation of body wave energy through the specimen-to-water interface, a decrease in crack-face noise, or a combination of these. In a different program, tests involving water did not show significant effect. A resolution of these differences is being investigated.

The specimen used for the water-effect tests was subsequently used to investigate the characteristics of oxide in a fatigue crack. An oxide was formed on the fatigue crack fracture surfaces by loading the specimen to open the crack, inserting a wedge to keep the crack open, and then immersing the

specimen in distilled water for about six weeks. AE was obtained during unload following wedge removal (Figure 16) and subsequent fatigue cycling (Figure 17), which produced approximately 1/4 in. of crack growth. When compared to AE from FCG in the same specimen prior to oxidation, the "oxide data" showed that the initial AE data rate in the absence of FCG was high relative to AE-FCG data obtained from unoxidized specimens. Once the fatigue crack front moved away from the oxidized fracture faces, the AE rate returned to levels similar to that obtained for FCG in air prior to oxidation.

A slag inclusion test specimen and an associated slag-free control specimen were fabricated from weld material provided from the GATX AE-weld monitor program. Both specimens were tested under cyclic loading with similar stress levels. The results (Figure 18) show that the average AE/cycle for the slag inclusion specimen was about 4-1/2 times that for the control specimen at the higher stress levels (3200 to 16,000 psi). The results are inconclusive, however, because:

- The AE signal parameters measured did not show any unique features or consistent pattern differences between the two specimens.
- The apparent slag inclusion was very small (approximately 0.015 in. diameter).
- An uncertainty exists as to how much of the flaw was slag inclusion versus void.
- Incomplete fusion along the loading axis of the slag inclusion specimen definitely occurred and may have had an effect on the results.

HIGH-TEMPERATURE AE SENSOR

The objective of high-temperature sensor testing is to test the feasibility of using available high-temperature AE sensors for continuous monitoring of reactor pressure boundaries. Three high-temperature sensors have been screened by laboratory testing at 550°F (288°C) with the expectation that development of a new high-temperature sensor concept could be avoided at least for the near future. The results to date are encouraging.

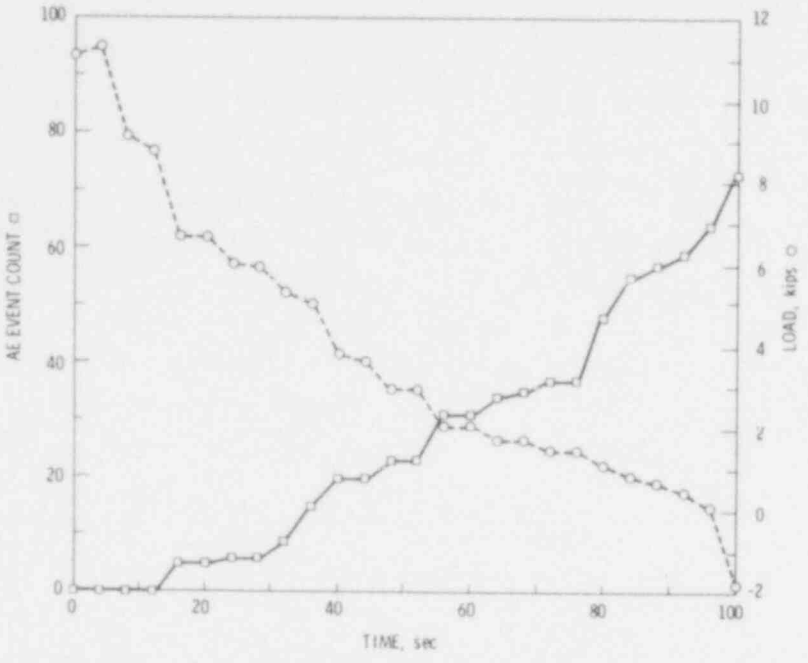

FIGURE 16. AE Count and Load Data Versus Time for DCB Specimen 1-2A-5A-4-Following a Six-Week Exposure in Room Temperature Distilled Water

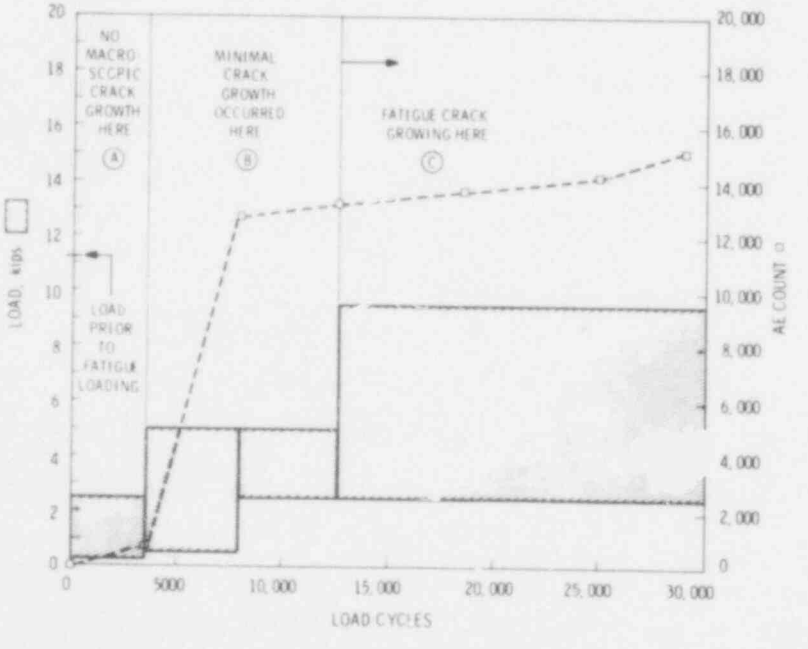

FIGURE 17. AE Count and Loading Range Data Versus Total Load Cycles for DCB Specimen 1-2A-5A-4 Following a Six-Week Exposure in Room Temperature Distilled Water

567 011

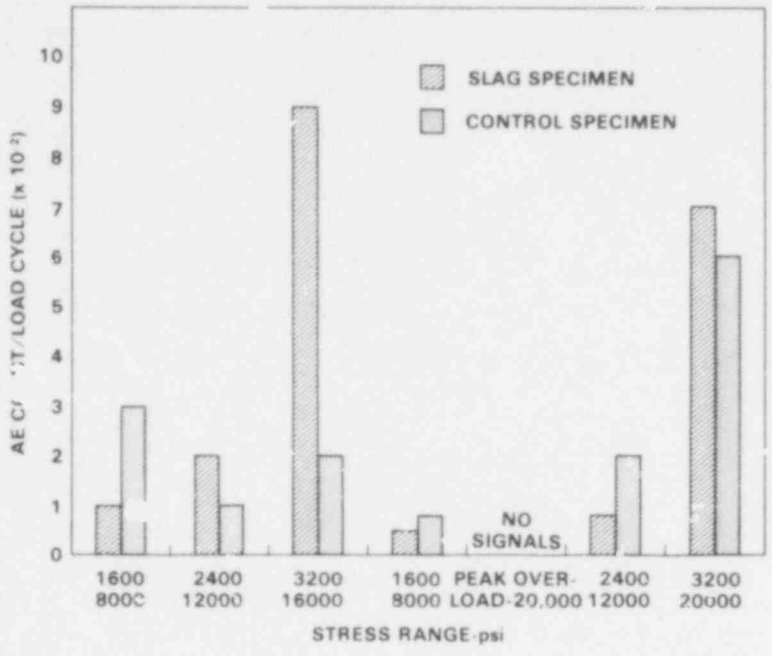

FIGURE 18. High Temperature Sensor Response to a Constant Pulse Input to Test Plate Measured at 550°F

The laboratory test procedure is to mount the sensors (dry pressure coupled) on an 8 by 11.5 by 1.5 in. (203 by 292 by 38 mm) A533B steel plate installed in a controlled temperature oven. The oven is heated to 550°F (288°C) continuously Monday through Friday and cooled to room temperature over the weekend. This cycle is repeated each week.

Two primary sets of data on sensor performance were taken--one on June 1, 1978, after approximately 1440 hr of exposure to 500° to 550°F (260 to 288°C) and the second on September 15, 1978 after approximately 2830 hr exposure. The methods used for both sets of data were similar. Pulse signals were generated electronically in the test plate using a high-temperature transducer mounted on the plate. Output signals from the test sensors were frequency filtered, using a Krohn-Hite Model 3202 dual-variable filter to produce data for varicus frequency high-pass categories. Sensor response results are shown in Figures 19 and 20. The June 1 measurements were made at room temperature to permit including a laboratory sensor for comparison. The September 15 measurements were made at 550°F 288°C).

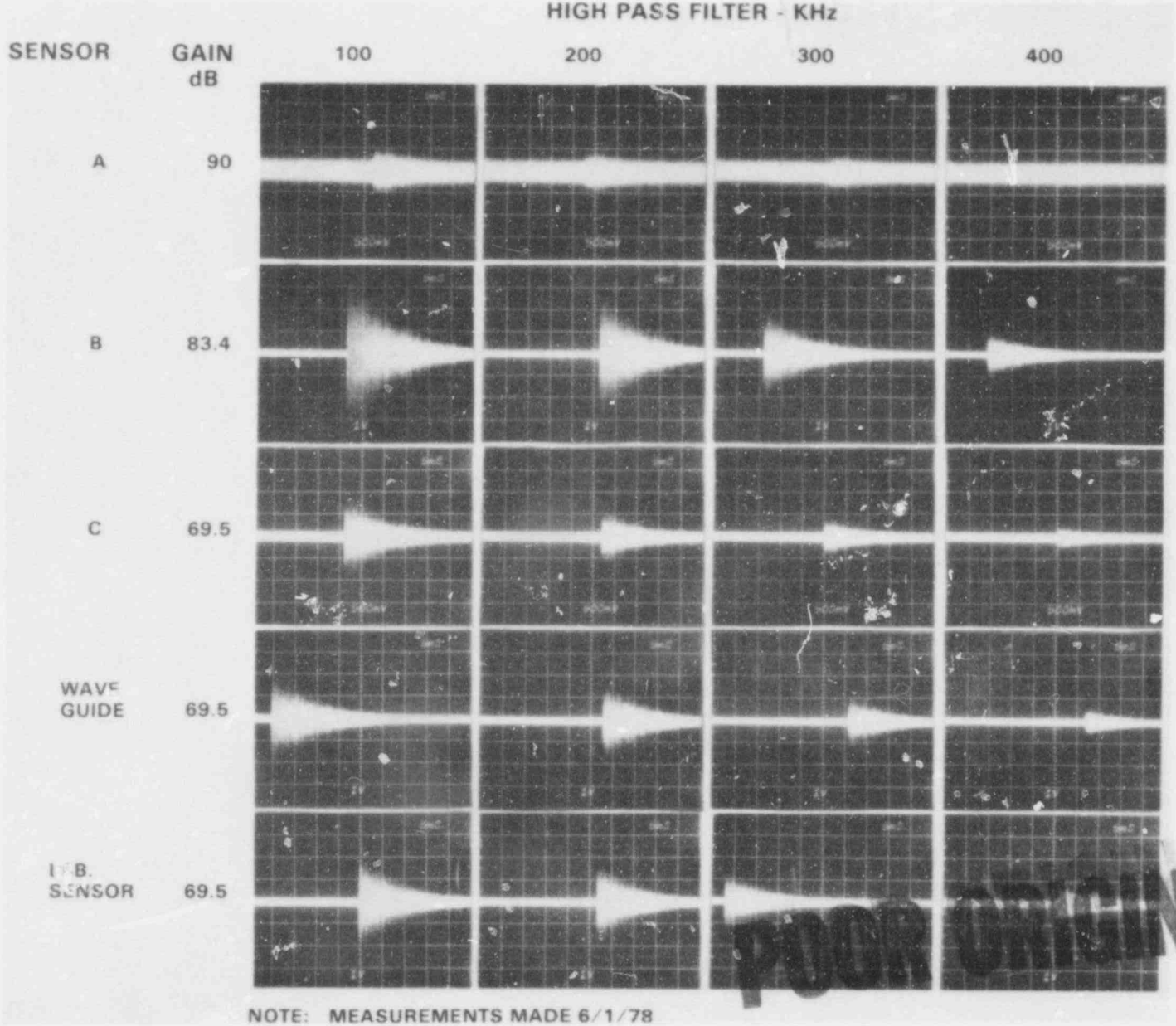

FIGURE 19. High Temperature Sensor Response to a Constant Pulse Input to Test Plate Measured at Room Temperature

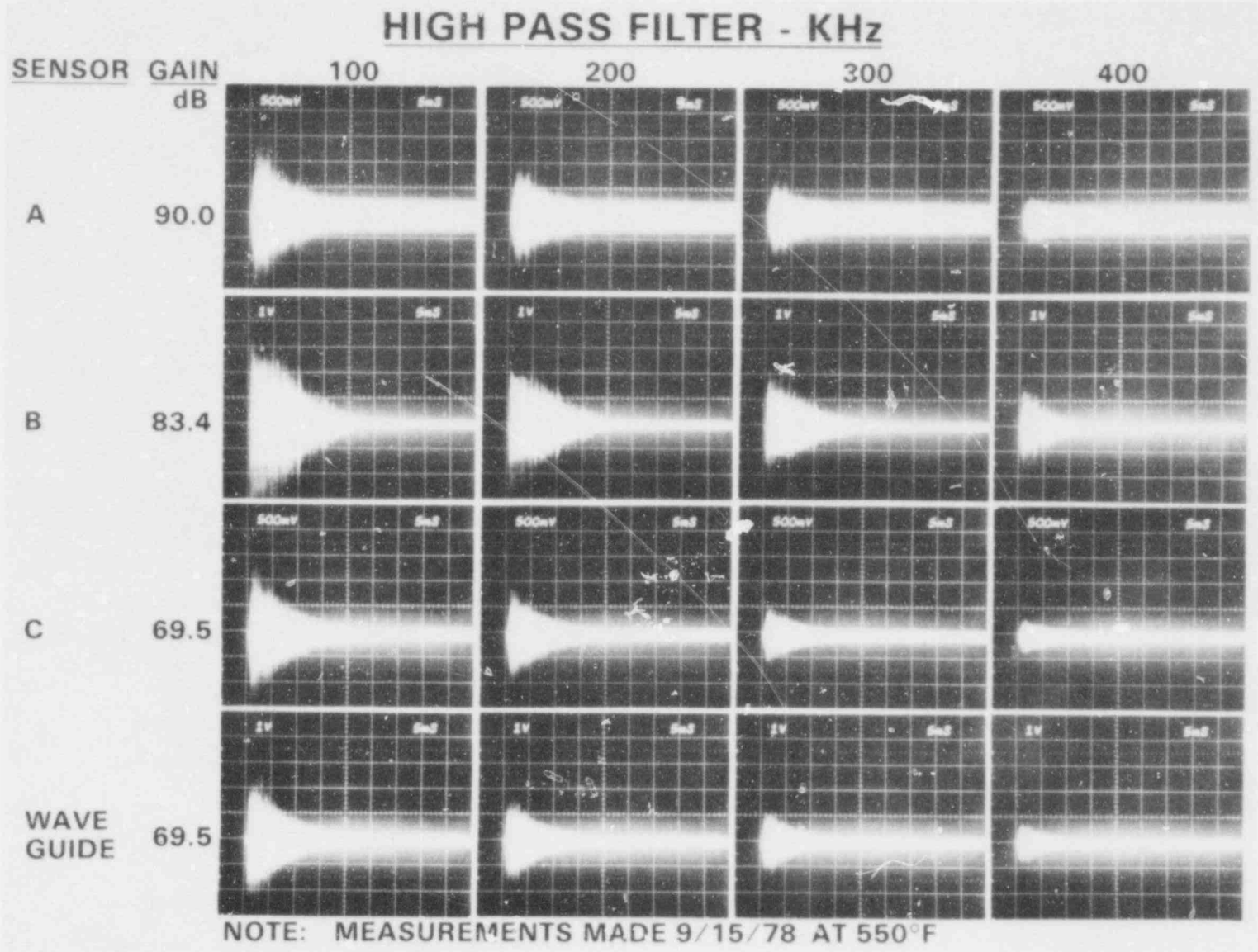

FIGURE 20. High Temperature Sensor Response to a Constant Pulse Input to Test Plate Measured at 550°F

One aspect of the data which was evaluated was the response versus increasing lower frequency limit. It appears that continuous monitoring of a vessel during operation would likely need to be done with a lower frequency limit of about 400 kHz to avoid hydraulic noise interference.

Another consideration examined was S/N ratio. S/N ratio is significant to any AE monitor system that utilizes a threshold limit for signal detection (nearly all current systems do). Table 3 gives the results of S/N ratio determination. Observations from these results are:

- The input signal in the 09/15/78 test may have been slightly stronger than in the 06/01/78 test; however, the 09/15/78 test was run at 550°F which may also contribute the stronger response in that test.
- Sensor B is very promising. It retains about 35% of its broadband sensitivity at the 400 kHz condition and the S/N ratio at 400 kHz is equal to that of the laboratory sensor. We consider this to be important to a field application consideration. An S/N ratio of less than 2 to 3 would be marginal.
- The metal wave guide represented in these tests is a concept long recognized as one method of AE monitoring a high-temperature surface. It has some disadvantage over a surface-mounted sensor (such as Sensor B). The wave guide will generally influence the character of the signal received out of the piezoelectric crystal at its outer end. To effectively protect the piezoelectric crystal from overheating, the wave guides are often several feet long, which makes them subject to physical damage. The wave guide is, however, a demonstrated method of detecting AE events from a high-temperature surface.
- Two sensor concepts--Sensor B and the metal wave guide--appear at this time to present viable methods of detecting AE on a reactor pressure vessel. The final test process will consist of exposing them to an actual reactor environment (temperature plus nuclear radiation). Arrangements for this are in progress.

TABLE 3. Signal-to-Noise Ratio for High-Temperature Sensors

06/01/78

Sensor	Gain, dB	High Pass Filter, kHz 100	200	300	400
A	90.0	2	1.4	1.1	--
B	83.4	20	15	11	6
C	69.5	7	5.6	4	1.6
Wave Guide	69.5	11	9	6	2.5
Lab Sensor	69.5	12	10	7.5	6

09/15/78

Sensor	Gain, dB	High Pass Filter, kHz 100	200	300	400
A	90.0	4.7	3.2	2.7	1.3
B	83.4	17.5	14.0	11.5	7.5
C	69.5	10.0	6.7	4.0	2.3
Wave Guide	69.5	12.0	7.2	5.2	3.2

AE/FLAW MODEL DEVELOPMENT

EMPIRICAL MODELS

Two empirical models have been used to describe fatigue crack growth data. The first model uses a power-law expression to relate the rate of change of AE variables to FCG parameters such as the stress intensity factor range (ΔK) and the crack growth rate (da/dn). The expression is typically of the form:

$$(dN/dn) = C_o (\Delta K)^m \quad (1)$$

where (dN/dn) represents the number of AE counts per cycle. Conceptually, this approach allows a direct assessment of flaw severity by measuring the AE count rate and temperature of the vessel (Figure 21). A knowledge of the flaw shape or the stress field in the vicinity of the suspected flaw should not be required. The influence of variables such as R ratio, cycle rate, service loadings, material volume, and possible flaw geometry effect are yet to be defined. The work scheduled for FY-79 is aimed at investigating the effect of these variables. In addition, the data scatter associated with the current rate model is typically quite large. More extensive characterization of the AE signals with respect to mechanical parameters such as the COD and the position of the signal on the load waveform may improve the rate analysis method.

The second technique for correlating AE-FCG data is to plot the total accumulated AE against either the stress intensity factor (K) or the crack opening displacement (COD). In this instance, the summation AE versus K or COD is usually linear and of the form:

$$\Sigma N = B_1 \ K + B_o \quad (2)$$

where B_1 and B_o are constants. This approach is attractive because of the reduced data scatter and linear behavior (see Figure 22). It may, however, require an initial definition of flaw shape and stress field once the AE

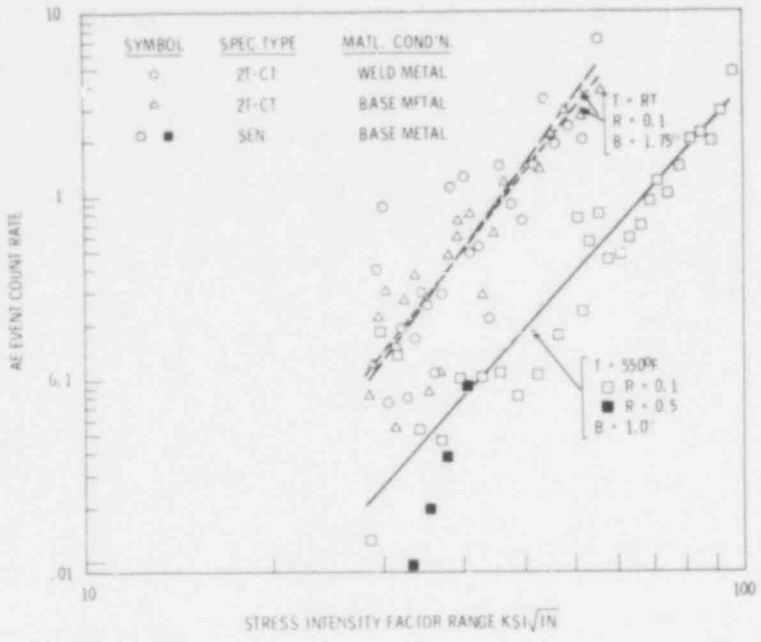

FIGURE 21. Composite AE Event Count Rate Versus ΔK Curves, Room Temperature and 550°F

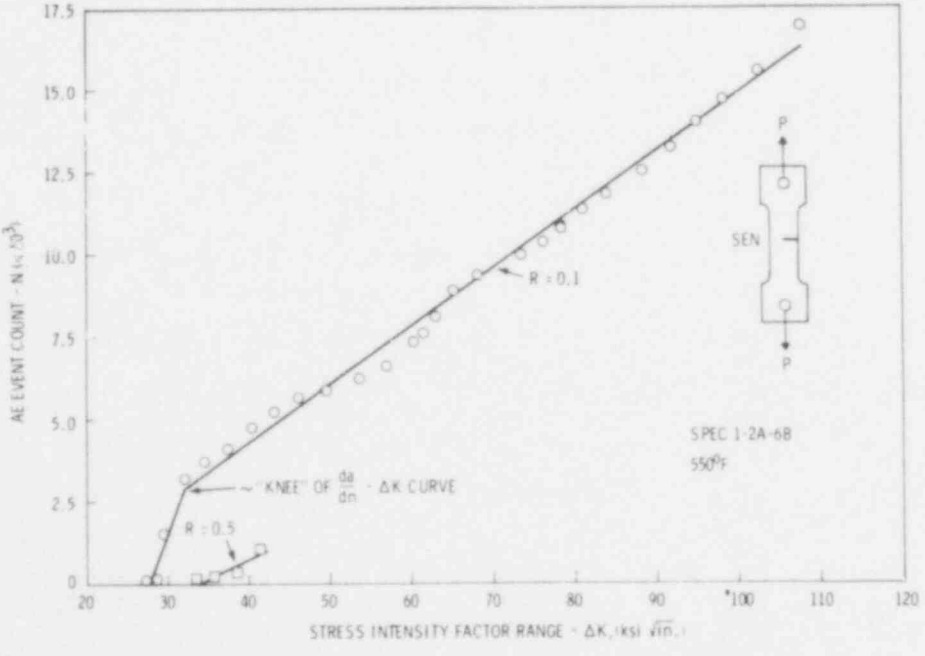

FIGURE 22. Summation AE Event Count Versus ΔK, Specimen 1-2A-6B, 550°F

indicates a growing flaw. Again, as with the rate method, the effects of variables such as load cycle rate, R-ratio, simulated service loading, material volume, and temperature must be further defined.

The AE obtained from fracture tests run on intermediate scale pressure vessels has been correlated with both K and COD. For two SN defect laboratory specimens, the results (Figures 11 and 12) have been correlated with COD only. No attempt was made to use K in laboratory specimen calculations due to the early onset of net section yielding.

HSST pressure vessel tests (Figures 13 and 14) have produced excellent results between summation AE and COD or K. In this case, the COD parameter was most effective at relating to the full range of the AE data. This result suggests that fracture mechanics variables which are sensitive to flaw plasticity may provide the best correlations with AE parameters.

THEORETICAL MODELS

Three theoretical models based upon linear elastic fracture mechanics were compared against the FCG results obtained from several different specimens. This section describes the models and compares the predicted results with the empirical results.

The first model[4-7] assumes that the number of AE events, N, detected during FCG is proportional to the change in the crack tip plastic zone volume:

$$dN = \alpha dVp \tag{3}$$

where α is a material constant and Vp is the plastic zone volume. The term Vp is estimated from the following expression:

$$Vp = B\pi\left(r_p\right)^2 = \frac{B}{4\pi(1-R)^4}\left(\frac{\Delta K}{\sigma_y}\right)^4 = C_o(\Delta K)^4 \tag{4}$$

where B is the specimen thickness, r_p is the plastic zone radius, R is the ratio of minimum to maximum load during FCG, σ_y is the yield strength, and C_o is a constant. A simple expression for ΔK may be written as:

$$\Delta K^2 \approx \Delta\sigma^2 \pi a \tag{5}$$

where σ is the difference between the maximum and minimum applied stress and a is the crack length. Substitution of Equation (5) into Equation (4) and differentiating leads to the following expression:

$$dVp \approx 2\pi C_o (\Delta\sigma)^2 (\Delta K)^2 da \tag{6}$$

Assuming that ΔK is constant for infinitesimal changes in crack length, and then substituting Equation (6) into Equation (3) and dividing both sides by the number of applied load cycles, dn, the following result is obtained:

$$dN/dn = 2\pi C_o \alpha(\Delta\sigma)^2 (\Delta K)^2 da/dn \tag{7}$$

This expression may be simplified by substituting the well known empirical equation relating da/dn and ΔK:

$$da/dn = C_1(\Delta K)^q \tag{8}$$

where C_1 and q are constants. Thus, the final equation relating dN/dn and ΔK is:

$$dN/dn \approx 2\pi C_o C_1 \alpha(\Delta\sigma)^2 (\Delta K)^{2+q} \tag{9}$$

The second theoretical model, which was originally proposed by Palmer, et. al.,[8,9] assumed that the number of AE events produced depends upon the change in crack tip plastic zone size rather than volume. This assumption may be expressed as:

$$dN = \beta dS_p \tag{10}$$

where β is considered to be a constant of proportionality depending on strain rate, temperature and microstructure. The linear elastic approximation for the plastic zone size is commonly taken to be:

$$S_p \approx 2B\pi r_p = C_2(\Delta K)^2 \tag{11}$$

where C_2 is a constant composed of terms defined above. Following a development similar to that used for the plastic zone volume derivation, another result is obtained for dN/dn:

$$dN/dn \approx \pi C_1 C_2 \beta(\Delta\sigma)^2 (\Delta K)^q \tag{12}$$

The last model that was reviewed is from Sinclair, et al.[10] This model is very interesting because of the experimental results that Sinclair, et al. used to support their theory. The AE data was obtained on A533B steel during FCG. In addition, the AE monitoring system utilized multisensor source isolation techniques to restrict the data to only those signals that originated in the vicinity of the flaw, and event count rather than ringdown count were measured. The methods used to obtain the AE were nearly equivalent to the techniques employed at PNL. The only significant difference was that Sinclair, et. al. used a voltage-controlled gate to restrict the detected emissions to those occurring during 80% of the upward part of the load cycle.

The basic assumption behind the model is that the total number of emission events, N, detected during cyclic loading in which fatigue crack area, A, is created is directly proportional to that area. In differential form this assumption may be expressed as:

$$dN = \Upsilon dA \tag{13}$$

where Υ is defined as the specific emission activity for FCG in the material under test. Since dA is equivalent to Bda we may rewrite Equation (13) to read:

$$dN = B\Upsilon da \tag{14}$$

Dividing both sides of Equation (14) by dn and substituting for da/dn, we have:

$$dN/dn = BYC_1(\Delta K)^q \qquad (15)$$

Theoretical equations relating summation AE (ΣN) to ΔK may be simply derived by integrating Equations (3), (10), or (13) for each respective model. A summary of the theoretical predictions and experimental results obtained from rate and summation analyses of several specimens is listed in Table 4. The total valid unpartitioned AE count was used for calculating the experimental dN/dn - ΔK and the ΣN - ΔK curves. In general, the compact tension rate data agree with the behavior predicted by the plastic zone and crack area models. The room temperature SEN rate data agree with the plastic zone and crack area models, but the 550°F SEN rate data agree with none of the models. In regard to the summation analysis predictions, none of the experimental results matched the theoretical calculations.

The reasons for the general lack of agreement between the theoretical and experimental calculations may, in part, be due to a breakdown of linear elastic fracture mechanics when applied to AE monitoring. Since fracture mechanics variables are based upon continuum mechanics concepts without regard to the microstructural nature of the material, it is not surprising to find

TABLE 4. Summary of AE-FCG Rate and Summation Analyses for Several Specimen Geometries and Material Conditions

	Plastic Zone Volume	Plastic Zone Size	Crack Area	Experimental Results
Rate dN/dn . $\propto$	ΔK^{q+2}	ΔK^q	ΔK^q	$\Delta K^{2.4-4.8}$
Summation $\Sigma N \propto$	ΔK	ΔK	ΔK	ΔK

NOTE: The exponent q is the exponent for the da/dn - ΔK power- law relation, and is typically in the range of 2.3 to 2.8 for values of ΔK between 20 and 100 ksi $\sqrt{in.}$

that attempts to correlate microscopic failure events (AE) with macroscopic measurements (i.e., loading state, crack length, COD, etc.) may only be partially successful. In addition, using the total valid unpartitioned AE count obtained from the entire load cycle may not be valid.

The possible combination of crack extension and crack closure emissions may tend to complicate analysis of the results. The data published by Sinclair, et al.[9] seem to indicate that this hypothesis has some merit. Part of the effort for FY-79 will concentrate on partitioning the AE with respect to position on the load waveform. Most likely this work will aid in clarifying the situation.

RECOMMENDATIONS FOR FUTURE WORK

Discussion of further development work is categorized relative to general program objectives.

AE/FLAW MODEL DEVELOPMENT

We feel that the two empirical models discussed in the preceding section demonstrate that an interpretive model is feasible. Although we recognize that the models are not yet adequately refined for application, it is important at this time to verify that the same response pattern can be observed under conditions simulating the major factors associated with on-reactor monitoring. Evident factors that require definition or further confirmation are the effects of load cycle rate, R-ratio, (minimum load/maximum load), simulated service loading, material volume, water and temperature.

The effect of load cycle rate is vital to determining if the denominator in the AE rate/crack growth rate model can be converted from load cycles to the more tractable parameter of time for inservice monitoring.

For practical reasons, FCG testing to date has been performed at low R-ratios. Since much of the cyclic loading on a reactor system will be at high R-ratio, it is necessary to now confirm whether this will influence the AE/flaw models.

Closely allied with consideration of high R-ratio is consideration of simulated reactor service loading. FCG studied so far on this program has been generated by constant amplitude sinusoidal cyclic loading. Testing which attempts to simulate service loading is needed to determine if this influences the AE/fracture mechanics relationship. Such a test might incorporate monotonically increasing load with a high R-ratio cyclic load superimposed during a prolonged hold at load, removing all load for a period, and then repeating the cycle.

Limitations of test equipment capacity have limited FCG testing to thicknesses of 1 to 2 in. Limited insight as to the effect of greater material

volume on detected AE has been gained from monitoring two HSST test vessels (6-in. wall) during fracture testing. Both vessel tests showed more AE in the elastic region than have laboratory fracture tests. Similar interfacing with other programs performing heavy section testing (preferably FCG should continue.

Comparison of results from laboratory fracture tests and HSST vessel tests shows tentative indication of a flaw geometry effect. An SN lab specimen test compared more closely with the vessel tests than did lab specimens using a through-wall notch. Further investigation of flaw geometry effect is planned using SN FCG specimens.

Empirical results concerning temperature effects on AE are inconsistent. Laboratory FCG tests have shown a reduction in AE in going from room temperature to 550°F. Conversely, HSST vessel and SN fracture tests showed effectively no effect on AE relative to fracture mechanics comparing -5° with +200°F. This inconsistency must be resolved.

Similarly, one FCG test of water effects using an immersed specimen showed a reduction in AE associated with immersion in water. Due to multiple possible causes, this result is not conclusive. Since fatigue cracks in a reactor vessel may be exposed to water, this question must be answered positively.

A test of path dependence during FCG, i.e., decreasing versus increasing ΔK, is planned as one test of the validity of the present AE/flaw model.

A test is needed to verify that the present AE/flaw model is discernable under the major conditions present in reactor monitoring. This may take the form of a cylindrical test specimen with an inside flaw exposed to pressurized, high-temperature water. The flaw would be grown by cyclic loading at low- and high-cycle rates and R-ratios.

AE SIGNAL CHARACTERIZATION

As discussed earlier in this report, work to date in the area of AE signal characterization to distinguish AE from other acoustic signals has not produced the results desired. It is vital that progress in this area be

emphasized. Two general avenues of investigation are planned. Using a recently assembled computer data analysis system, we plan a more rigorous analysis of the measured AE parameters. This includes such parameters as energy, a modified peak-time and peak-amplitude measure, and first half-cycle polarity. Also, a new parameter is now available for FCG studies. This consists of identifying the time location of each valid AE signal with respect to the load waveform. This offers new potential for relating to the details of FCG and identifying the possible contribution of crack interface noise to the total AE measured from a growing crack.

A second avenue of investigation is to further explore pattern recognition techniques for identifying AE signals. Recent work applying pattern recognition to eddy current and ultrasonic signals and a very limited sample of AE signals has produced encouraging results. We plan to collect samples of valid AE signal waveforms in digital form during crack growth, slag inclusion and oxide tests. Samples of known and identified noise signals (tapping and rubbing on the specimen and electrical transients, etc.) will also be provided. These will then be examined by pattern recognition techniques for distinguishing features.

DATA ACQUISITION SYSTEM

The AE sensor is obviously the key element in a data acquisition system. High-temperature AE sensors have been tested in the laboratory for nearly a year. At least one sensor shows good resistance to temperature exposure (550°F and 288°C). Testing now needs to be expanded to actual reactor environment (temperature, humidity and radiation exposure).

APPLICATION DEMONSTRATION

Two interrelated efforts are required in preparation for demonstration of program results. One of the efforts concerns development and design of an optimized on-reactor AE data acquisition system. Considerations to be taken into account include:

- total volumetric monitoring versus selected area (welds, nozzles, etc.) monitoring
- AE source determination method, i.e., identify an area by source isolation, a resolution element pattern using "look-up" tables in a computer, or point source determination on each signal
- data recording and readout method.

Related to the data acquisition system design is design of a methodology for application of an interpretive model in the field. This will have a direct bearing on design of the data processing portion of the data acquisition system.

A minimum of about two years of on-reactor monitoring will be required to demonstrate the results of this program and overcome practical problems expected to surface during such a test phase.

DETERMINATION OF AE SOURCE MECHANISMS

Although it is outside the scope of this program, investigation of AE source mechanisms could aid the development of analytical relationships between AE detected during structural FCG and the severity of the flaws producing AE. Such investigations could provide a basis for selecting appropriate engineering parameters for use in model development.

Additionally, this work could provide a means for making rational predictions on conditions that might occur on a structure, but which were not tested in the laboratory. Laboratory experiments, as a matter of economics, cannot test all possible combinations of variables (e.g., R-ratio, cycle rate, radiation effects and water pressure and temperature) which might influence the AE during reactor operation. However, when theoretical concepts are merged with appropriate experimental measurements the "gaps" in the data are closed.

In addition, such work might also shed some light on the nature of basic deformation and fracture events that accompany subcritical crack initiation and propagation. Although much work has been done in this area there is still relatively little known about the micromechanics of these processes.

REFERENCES

1. Hutton, P. H, C. B. Schwenk, R. J. Kurtz and C. Pavloff. Acoustic Emission--Flaw Relationships for In-Service Monitoring of Nuclear Pressure Vessels. Annual Report No. 1, NUREG 0250-3, BNWL-2232-3, Pacific Northwest Laboratory, Richland, WA.

2. Hutton, P. H., J. F. Dawson and R. J. Kurtz. 1978. Appendix B in Test of Six-Inch-Thick Pressure Vessels, Series 3: Intermediate Test Vessel V-78. NUREG/CR-0309, ORNL/NUREG-38, Oak Ridge National Laboratory, Oak Ridge, TN.

3. Hutton, P. H., E. B. Schwenk and R. J. Kurtz. 1979. "Acoustic Emission--Flaw Relationships for In-Service Monitoring of Nuclear Pressure Vessels." In Reactor Safety Research Programs Quarterly Report, July 1--September 30,1978. NUREG/CR-0546, PNL-2653-3, Pacific Northwest Laboratory, Richland, WA.

4. Morton, T. M., R. M. Harrington and J. G. Bjeletich. 1973. Eng. Frac. Mech., 5:691.

5. Harris, D. O, and H. L. Dunegan. 1974. Exp. Mech., 14:71.

6. Morton, T. M., S. Smith and R. M. Harrington. 1974. Exp. Mech., 14:208.

7. Lindley, T. C., I. G. Palmer and C. E. Richlard. 1978. Matl. Sci. Eng., 32:1.

8. Palmer, I. G. and P. T. Heald. 1973. Matl. Sci. Eng., 11:181.

9. Palmer, I. G. 1973. Matl. Sci. Eng., 11:227.

10. Sinclair, A. C. E. , D. C. Connors and C. L. Formby. 1977. Matl. Sci. Eng., 28:263.

NUREG/CR-0800
PNL-2977
R5

DISTRIBUTION

No. of
Copies

OFFSITE

A. A. Churm
DOE Chicago Patent Group
9800 S. Cass Avenue
Argonne, IL 60439

265 Basic Distribution Under
NRC R5

2 DOE Technical Information
Center

25 National Technical Information
Service

10 J. Muscara
Reactor Safety Research Division
Nuclear Regulatory Commission
Washington, DC 20555

2 Electric Power Research Institute
3212 Hillview Avenue
P.O. Box 10412
Palo Alto, CA 94304
L. Agee
B. R. Sehgal

F. Shakir
Department of Metallurgy
Association of American Railroads
3140 S. Federal
Chicago, IL 60616

SM-ALC/MMET
Attn: Capt. John Rodgers
McClellan AFB, CA 95652

Dr. Sotirios J. Vahaviolos
Western Electric, ERC
P.O. Box 900
Princeton, NJ 08540

Mr. Jerry Whittaker
Union Carbide Company
Oak Ridge National Laboratories
Y-12
Oak Ridge, TN 37830

Mr. L. J. Anderson, B2402
Dow Chemical Company
Texas Division
P.O. Drawer K
Freeport, TX 77541

Mr. M. C. Jor
Western Electric, ERC
P.O. Box 900
Princeton, NJ 08540

P. Caussin
Vincotte
1640 Rhode-Saint-Genese
Belgium

143 U.S. Acoustic Emission Working
Group Membership - labels
attached.

Don Birchon
Admiralty Materials Laboratory
Holton Health Poole
Dorser, England
020-122-2711

567 052

ONSITE

32 Pacific Northwest Laboratory

J. F. Dawson
A. J. Haverfield
J. L. Hooper
P. H. Hutton (15)
R. J. Kurtz
R. T. Landsiedel
R. P. Marshall
R. D. Nelson
N. J. Olson
G. J. Posakony
E. B. Schwenk (2)
J. R. Skorpik
Technical Information (3)
Publishing Coordination (2)